ICARUS 114, 33–50 (1995)

Secular Resonances in Mean Motion Commensurabilities: The 4/1, 3/1, 5/2, and 7/3 Cases

MICHÈLE MOONS

Département de Mathématique FUNDP, 8, Rempart de la Vierge, B-5000 Namur, Belgium

AND

ALESSANDRO MORBIDELLI

URA 1, Observatoire de la Côte d'Azur, B.P. 229, 06304 Nice Cedex 4, France

Received March 10, 1994; revised September 26, 1994

With this paper we complete our review on the dynamics in mean motion resonances. Here we investigate the 4/1, 3/1, 5/2, and 7/3 commensurabilities and show that, due to the interaction between the ν_5 and ν_6 secular resonances, chaotic motion is present almost everywhere in the phase space. This chaotic motion is responsible for the large jumps in the eccentricity (up to 0.8 or more) that one usually observes in the realistic numerical simulations, which force the asteroids to cross the orbits not only of Mars, but even of Earth. In this way we achieve a better understanding of the effective mechanisms for the depletion of the 3/1, 5/2, and 4/1 resonances, and we are able to explain, for the first time, the existence of the gap associated with the 7/3 mean motion commensurability.

1. INTRODUCTION

Up to now all previous analytic works on mean motion commensurabilities were developed within the simple framework of the planar elliptic restricted problem; conversely, many numerical works have been conducted within the framework of more realistic models, giving results which cannot be interpreted on the basis of the theories (for a review on mean motion resonances, see Froeschlé and Greenberg (1989)).

In our theoretic perturbation approach we investigate the secular motion in 3-D space within the framework of the Sun–Jupiter–Saturn–asteroid model, therefore taking account of the relevant role played by secular resonances *inside* mean motion commensurabilities. In this way, we are able to understand the dynamics observed in the realistic numerical simulations.

We recall that the secular resonances are the commensurabilities among the precession rates of the asteroid orbit and the precession rates of the planetary orbits. In particular the ν_5 (respectively, ν_6) resonance is given by the 1/1 commensurability between the frequency of the longitude of perihelion of the asteroid and the average frequency g_5 (respectively, g_6) of Jupiter's (respectively, Saturn's) longitude of perihelion. The ν_{16} resonance is the corotation of the node of the asteroid with that of Jupiter. In the classical restricted three-body problem, the ν_5 secular resonance is approximated by the resonance that occurs when the frequency of the asteroid's perihelion is locked around 0. Conversely, the other secular resonances are completely absent, since the orbit of Jupiter is assumed to be fixed.

The present work is the logical completion of our previous paper (Morbidelli and Moons 1993) devoted to the 3/2 and 2/1 mean motion commensurabilities. There, we found that, concerning the 3/2 mean motion commensurability, the interaction between the ν_5 and ν_6 secular resonances generates a wide chaotic region which bounds the eccentricities of the Hilda group in the (a, e) plane, while the ν_{16} resonance marks its boundary in the (e, i) plane. Conversely, in the 2/1 mean motion commensurability, the location of secular resonances is different, and a group like that of the Hilda's would be crossed (instead of bounded) by the ν_{16} secular resonance. However, this fact is not enough to explain the Hecuba gap completely, since the ν_{16} resonance does not much influence the behavior of the eccentricity. One could conjecture the existence of slow chaotic diffusion associated with higher order secular and secondary resonances, but this has not yet been proved.

Concerning the mean motion commensurabilities we investigate here, the existence of the gaps associated with the 4/1, 3/1, and 5/2 resonances is usually considered

0019-1035/95 $6.00

as a solved problem. As a matter of fact, since these commensurabilities occur in the inner part of the asteroid belt, it is enough to show that the eccentricity is temporarily forced up to moderate values to invoke depletion mechanisms due to close encounters with Mars. This is what was done first by Wisdom (1985) for the 3/1 and by Yoshikawa (1989, 1991) for the 4/1 and 5/2 within the framework of the simple model of the planar restricted three-body problem. However, we stress that this simple approach is not completely satisfactory. Indeed, explaining a hypothetical mechanism for the origin of the gap is not enough; one should be able to understand the dynamical behaviors usually observed in realistic numerical simulations which take the full Solar System into account. Now, the depletion of the gap due to temporary Mars-crossing, as proposed by Wisdom, would be efficient on a typical time scale of 100 myr. Conversely, the numerical simulations (see, for instance, Farinella *et al.* (1993), Froeschlé *et al.* (1995), Morbidelli and Moons (1995)) show that the eccentricity behaves very chaotically, with jumps to 0.8 or even larger values; therefore, the asteroid becomes an Earth-crosser and is ejected from the resonance on a typical time scale of 1 myr only.

In this paper we show that the interaction between the ν_5 and the ν_6 secular resonances generates wide and wild chaotic regions which cover most of the phase space. In particular, in these chaotic regions, the eccentricity is free to jump to relevant values, even larger than 0.8, as observed in the numerical simulations. The time scale of this phenomenon is typical of secular dynamics, i.e., 1 myr.

As a matter of fact, in some cases these chaotic regions generated by the interaction between ν_5 and ν_6 do not attain orbits with small eccentricity. However, we are confident that the presence of secondary resonances among the several degrees of freedom, as well as the small "kicks" provided by temporary Mars-crossing, can extend the chaotic regions almost everywhere, so that any orbit can wander all over the full range of eccentricity. We will provide a numerical example of this fact in the frame of the 5/2 commensurability in Section 6.

For what concerns the 7/3 mean motion commensurability, the approach based on the restricted three-body problem, as in Yoshikawa (1989, 1991), fails to explain the existence of the evidently associated gap. Here, we show that, again, the interaction between the main secular resonances ν_5 and ν_6 creates a chaotic layer which extends all over the phase space. The eccentricity can increase up to 0.7, which is an Earth-crossing value, so that the 7/3 commensurability is quickly depleted.

In light of these results, we can therefore state that the consideration of a more realistic model, which includes the secular motion of Jupiter, changes also from the qualitative point of view the usual results provided by the three-body model and allows a deeper understanding of the observed (simulated) phenomena.

We also stress that our perturbation approach, based on the introduction of Arnold action-angle variables and on the successive elimination of harmonics, makes it possible to investigate all the mean motion resonances without adaptive arrangements. This is particularly satisfactory from a mathematical viewpoint, but is a nonnegligible feature also from an astronomical viewpoint, since it makes possible a straightforward comparative study of all mean motion commensurabilities in the main asteroid belt.

The remainder of this paper is structured as follows. Section 2 is devoted to recalling the general settings and the perturbation approach already described in our previous paper (Morbidelli and Moons 1993) in a more detailed way. This section, important only from a mathematical viewpoint, can be skipped in order to go directly to Section 3, which discusses the common aspects of the dynamics in the different commensurabilities. The next sections are devoted to a more specific discussion on the 4/1, 3/1, 5/2, and 7/3 commensurabilities. We point out that, in contrast to our previous paper, we restrict our study to the planar case only, since the dynamics turns out to be chaotic already without introducing the third degree of freedom associated with the inclination.

2. RECALL OF THE GENERAL SETTINGS AND OF THE PERTURBATION SCHEME

Our approach, presented in detail in (Morbidelli and Moons 1993), is based on the philosophy of the successive elimination of perturbation harmonics (Morbidelli 1993) and makes use of the Henrard's seminumerical first-order perturbation method (Henrard 1990). For the reader's convenience, and in order to provide a self-contained paper, we will recall here the different steps of the theory we have constructed. This will be done without entering into details as these can be found in Morbidelli and Moons (1993).

We start with the Hamiltonian of the restricted three-body Sun–Jupiter–asteroid problem (see, for instance, Szebehely (1967))

$$\mathcal{H} = L' - \frac{1-\mu}{2a} - \mu\left(\frac{1}{|\mathbf{r}-\mathbf{r}'|} - \frac{\mathbf{r}\,|\,\mathbf{r}'}{r'^3}\right), \qquad (1)$$

where $\mathbf{r}$ is the heliocentric position vector of the asteroid, $\mathbf{r}'$ that of Jupiter, μ the mass of Jupiter, and L' the conjugate momentum to the mean longitude of Jupiter. In what follows we will adopt the usual notations for the Keplerian elements of the asteroid (respectively, Jupiter): a (respectively, a') for the semimajor axis, e (respectively, e') for the eccentricity, i (respectively, i') for the inclination, λ

(respectively, λ') for the mean longitude, $\tilde{\omega}$ (respectively, $\tilde{\omega}'$) for the longitude of perihelion, and Ω (respectively, Ω') for the longitude of node. We will also use the usual Delaunay's momenta: $L = \sqrt{(1-\mu)a}$, $G = L\sqrt{1-e^2}$, and $H = G\cos i$. The universal gravitational constant, the semimajor axis of Jupiter, and the total mass of the Sun–Jupiter system are chosen as units.

We immediately extend the problem by taking account of the changes in orbital parameters of Jupiter due to the presence of Saturn. This is achieved by incorporating the most important terms of the synthetic theory of Jupiter Longstop1B (Nobili *et al.* 1989) into our theory:

$$\begin{aligned} e'\cos\tilde{\omega}' &= m_{5,5}\cos(g_5 t + \lambda_5^0) + m_{5,6}\cos(g_6 t + \lambda_6^0),\\ e'\sin\tilde{\omega}' &= m_{5,5}\sin(g_5 t + \lambda_5^0) + m_{5,6}\sin(g_6 t + \lambda_6^0),\\ \sin\frac{i'}{2}\cos\Omega' &= n_{5,6}\cos(s_6 t + \mu_6^0),\\ \sin\frac{i'}{2}\sin\Omega' &= n_{5,6}\sin(s_6 t + \mu_6^0). \end{aligned} \tag{2}$$

By introducing variables appropriate to $(p+q)/p$ a mean motion resonance and averaging with respect to the short periodic oscillations (mean longitude of Jupiter), we end up with the six-degree-of-freedom Hamiltonian

$$\begin{aligned} \mathcal{H} = {} & g_5\Lambda_5' + g_6\Lambda_6' + s_6\Lambda_{16}'\\ & - \frac{p+q}{p}L - \frac{1-\mu}{2a} - \mu\left\langle \frac{1}{|\mathbf{r}-\mathbf{r}'|} - \frac{\mathbf{r}\,|\,\mathbf{r}'}{r'^3}\right\rangle, \end{aligned} \tag{3}$$

where $\langle . \rangle$ denotes the average over λ' and the phase space variables are

$$\begin{aligned} \sigma &= \frac{p+q}{q}\lambda' - \frac{p}{q}\lambda - \tilde{\omega}, & S &= L - G,\\ \sigma_z &= \frac{p+q}{q}\lambda' - \frac{p}{q}\lambda - \Omega, & S_z &= G - H,\\ -\nu &= \frac{p+q}{q}\lambda' - \frac{p}{q}\lambda, & N &= \frac{p+q}{p}L - H,\\ \tilde{\omega}_5' &\equiv g_5 t, & \Lambda_5', &\\ \tilde{\omega}_6' &\equiv g_6 t & \Lambda_6', &\\ \Omega' &\equiv s_6 t, & \Lambda_{16}'. & \end{aligned} \tag{4}$$

The averaged Hamiltonian (3) is composed of a main part $\mathcal{H}_0(\sigma, S, \sigma_z, S_z, N)$ and a perturbation $\mathcal{H}_1(\sigma, S, \sigma_z, S_z, \nu, N, \tilde{\omega}_5', \tilde{\omega}_6', \Omega')$, which contains the terms proportional to e' and i'. This Hamiltonian is neither expanded in power series with respect to the eccentricity and the inclination of the asteroid nor in Fourier series with respect to the asteroidal angular variables; its value, and the value of its derivatives, are numerically computed very precisely for any given value of the phase space variables using regular variables, as in (Ferraz-Mello and Sato 1989). In order to prevent from any confusion, we make clear that we do not perform the final expansion about the libration center given in that paper. The theory is thus valid for any value of the eccentricity and/or the inclination of the asteroid as well as for any value of the critical angles. The perturbation $\mathcal{H}_1$, on the other hand, is truncated at the first order in e' and i':

$$\begin{aligned} \mathcal{H}_1 = {} & m_{5,5}\mathcal{H}_{1,5}(\sigma, S, \sigma_z, S_z, \nu, N, \tilde{\omega}_5')\\ & + m_{5,6}\mathcal{H}_{1,6}(\sigma, S, \sigma_z, S_z, \nu, N, \tilde{\omega}_6')\\ & + n_{5,6}\mathcal{H}_{1,16}(\sigma, S, \sigma_z, S_z, \nu, N, \Omega'). \end{aligned} \tag{5}$$

In order to study the dynamics associated with the Hamiltonian (3), we look in the different regions of the phase space for the harmonics with the predominant effect and we proceed to their elimination like in (Morbidelli 1993); finally, we apply the Henrard's seminumerical first-order perturbation method (Henrard 1990).

2.1. *Reduction to the Planar Problem*

As announced in the introduction, we restrict our approach in this paper to the planar problem where we impose $i = i' \equiv n_{5,6} = 0$. In this case, the Hamiltonian (3) is reduced to

$$\begin{aligned} \mathcal{H} = {} & g_5\Lambda_5' + g_6\Lambda_6' + \mathcal{H}_0(\sigma, S, N)\\ & + m_{5,5}\mathcal{H}_{1,5}(\sigma, S, \nu + \tilde{\omega}_5', N)\\ & + m_{5,6}\mathcal{H}_{1,6}(\sigma, S, \nu + \tilde{\omega}_6', N), \end{aligned} \tag{6}$$

whose main part $\mathcal{H}_0$ is integrable but highly nonlinear (see, for instance, Henrard and Lemaitre (1983), Lemaitre (1984), Moons and Morbidelli (1993)).

We introduce suitable action-angle variables for $\mathcal{H}_0$ (Henrard 1990)

$$\begin{aligned} \psi &= \frac{2\pi}{T}t, & J &= \frac{1}{2\pi}\oint S\,d\sigma,\\ \psi' &= \nu - \rho(\psi, J, J'), & J' &= N, \end{aligned} \tag{7}$$

which can be evaluated numerically for each periodic trajectory of $\mathcal{H}_0(\sigma, S, N)$, T being the period of the trajectory and ρ a periodic function.

With this choice of variables, the Hamiltonian (6) is reduced to

$$\begin{aligned}\mathcal{H} &= g_5\Lambda_5' + g_6\Lambda_6' + \mathcal{H}_0(J, J') \\ &+ m_{5,5}\mathcal{H}_{1,5}(\psi, J, \psi' + \tilde{\omega}_5', J') \\ &+ m_{5,6}\mathcal{H}_{1,6}(\psi, J, \psi' + \tilde{\omega}_6', J'),\end{aligned} \tag{8}$$

the unperturbed frequencies of the system being given by

$$\omega_1 = \dot{\psi} = \frac{\partial \mathcal{H}_0}{\partial J} = \frac{2\pi}{T}, \quad \omega_2 = \dot{\psi}' = \frac{\partial \mathcal{H}_0}{\partial J'} = \frac{1}{T}\int_0^T \frac{\partial \mathcal{H}_0}{\partial N}\, dt. \tag{9}$$

In order to locate the secular resonances ν_5 and ν_6 introduced by the perturbation, we compute the level curves $\omega_2 = -g_5$ and $\omega_2 = -g_6$ in the (a, e) plane as functions of the initial conditions of integration $(a, e, \sigma = \sigma^*)$, σ^* being the value of σ at the stable equilibrium point of the first degree of freedom ($\sigma^* = 0$ for the 3/2, 2/1, 5/2, and 4/1 resonances; $\sigma^* = \pi/4$ for the 7/3 resonance; $\sigma^* = \pi/2$ for the 3/1 resonance). Results have been presented in Moons and Morbidelli (1993) and are reproduced here in Figs. 2, 6, 10, and 15 for the 4/1, 3/1, 5/2, and 7/3 mean motion commensurabilities. In these figures, the solid bold curve corresponds to the ν_5 secular resonance and the dashed bold curve to the ν_6 secular resonance. As shown in these figures, the two secular resonances ν_5 and ν_6 are relatively close to each other in general.

Moreover, we have also computed in the (a, e) plane the level curves $\omega_2/\omega_1 = j$ in order to locate the secondary resonances introduced by the perturbation. In the 4/1, 5/2, and 7/3 cases, they seem to be embedded in a zone very near the separatrix of the first degree of freedom. In the 3/2, 2/1, and 3/1 cases, on the contrary, they appear clearly at the center of the resonance, but for small to moderate values of the eccentricity, very far from the zone where the secular resonances ν_5 and ν_6 are found; these results have already been published in Moons and Morbidelli (1993) and are not reproduced here.

The fact that ψ is a much faster variable than ψ' in the region of the phase space near the secular resonances allows us to average the Hamiltonian (8) with respect to ψ. Introducing the canonical change of variables (the momentum Π' is constant)

$$\begin{aligned} &\psi, && J \\ &\psi', && \Pi' = J' - \Lambda_5' - \Lambda_6' \\ &\psi_5' = \psi' + \tilde{\omega}_5', && \Lambda_5' \\ &\psi_6' = \psi' + \tilde{\omega}_6', && \Lambda_6' \end{aligned} \tag{10}$$

and using the seminumerical first-order method of Henrard (1990), we then get the two-resonance model Hamiltonian

$$\begin{aligned}\overline{\mathcal{H}} &= g_5\overline{\Lambda}_5' + g_6\overline{\Lambda}_6' + \overline{\mathcal{H}}_0(\bar{J}, \bar{J}') \\ &+ m_{5,5}\overline{A}_5(\bar{J}, \bar{J}')\cos(\bar{\psi}_5' + \sigma^*) \\ &+ m_{5,6}\overline{A}_6(\bar{J}, \bar{J}')\cos(\bar{\psi}_6' + \sigma^*),\end{aligned} \tag{11}$$

where the action $\bar{J} = J + O(e')$ is now an integral of motion. The coefficients $\overline{A}_i(\bar{J}, \bar{J}')$ are such that

$$\begin{aligned}&\overline{A}_i(\bar{J}, \bar{J}')\cos(\bar{\psi}_i' + \sigma^*) \\ &\qquad = \overline{B}_i(\bar{J}, \bar{J}')\cos\bar{\psi}_i' + \overline{C}_i(\bar{J}, \bar{J}')\sin\bar{\psi}_i',\end{aligned} \tag{12}$$

where

$$\begin{aligned}\overline{B}_i(\bar{J}, \bar{J}') = \frac{1}{T}\int_0^T \mathcal{H}_{1,i}(\sigma(t), S(t), \nu(t) - \omega_2 t, \\ N(t), \tilde{\omega}_i' = 0)\, dt.\end{aligned} \tag{13}$$

The integral is computed along the periodic trajectories of $\mathcal{H}_0$ as in (7), the initial condition $\nu(0)$ being 0. The coefficients $\overline{C}_i(\bar{J}, \bar{J}')$ are also given by the integral (13) but with the initial condition $\nu(0) = \pi/2$.

As said previously, the two secular resonances ν_5 and ν_6 are relatively close to each other. On first making an approximation, however, and in order to have an idea of their extent by means of a semianalytical theory, we will consider these resonances separately, taking one of them into account while neglecting the other one and vice versa. This will lead us to study the two-degree-of-freedom integrable Hamiltonian

$$\overline{\mathcal{H}}_i = g_i\bar{J}' + \overline{\mathcal{H}}_0(\bar{J}, \bar{J}') + m_{5,i}\overline{A}_i(\bar{J}, \bar{J}')\cos(\bar{\psi}_i' + \sigma^*), \tag{14}$$

describing the secular dynamics associated with ν_i in the plane.

We have computed the location of the separatrices of (14) for different levels $J = C'$ as well as their traces in the plane $(a, e, \sigma = \sigma^*, \psi_i' = \psi^*)$, ψ^* being the value of ψ_i' corresponding to the stable equilibrium point of (14). For the 3/1 mean motion commensurability, the traces of the separatrices, computed from the two independent models, are shown in Fig. 6: continuous lines for the separatrices of the ν_5 secular resonance and dashed lines for the separatrices of the ν_6 secular resonance. Results for the 4/1, 3/1, 5/2, and 7/3 commensurabilities are discussed in detail in the next sections. As in the 2/1 and the 3/2 cases (see Morbidelli and Moons (1993)), we find a very wide overlapping region of the two secular resonances and, therefore, the approximation we have made in studying ν_5 while neglecting ν_6 (or vice versa) is here also too crude.

In order to have a realistic model of the dynamics in

the region of the $\nu_5 + \nu_6$ secular resonances, we thus must consider the whole two-resonance model Hamiltonian (11). This Hamiltonian has been integrated numerically and the results are discussed in the next sections.

3. SECULAR DYNAMICS IN MEAN MOTION COMMENSURABILITIES: COMMON ASPECTS

This section describes the common features of the dynamics in the mean motion resonances and explains the meaning of the figures presented in the next sections.

In a first approximation, we assume the orbit of Jupiter to be circular, thus considering the eccentricity of Jupiter as a perturbation parameter. From the physical point of view, this is justified by the fact that the motion described by the circular problem is the one with the shortest time scale. Moreover, we restrict our analysis to the plane of Jupiter's orbit.

After averaging over the mean longitude of Jupiter (λ'), the *planar* circular problem is integrable. For our purposes here it is sufficient to recall that the dynamics described by the averaged planar circular problem has a constant of motion

$$N = \sqrt{(1-\mu)a}\left(\frac{p+q}{p} - \sqrt{1-e^2}\right), \qquad (15)$$

where a and e are the semimajor axis and the eccentricity of the asteroid. Figures 1, 5, 9, and 14 show the curves N equal constant in continuous lines. Moreover, in these figures, the central bold line denotes the main stable family of equilibrium points. The two thick lines on the sides of each figure denote the separatrices, which can be considered as the real bounds of the mean motion resonance in consideration. Indeed the critical angle of the resonance, i.e.,

$$\sigma = \frac{p+q}{q}\lambda' - \frac{p}{q}\lambda - \tilde{\omega},$$

(λ and $\tilde{\omega}$ being the mean longitude and the longitude of perihelion of the asteroid) librates for all orbits under initial conditions at $\sigma = \sigma^*$ in between the two thick lines ($\sigma^* = 0$ for the 5/2 and the 4/1 resonances, $\sigma^* = \pi/4$ for the 7/3 resonance, and $\sigma^* = \pi/2$ for the 3/1 resonance). For these orbits, a and e oscillate, together with the libration of σ, on a line N = constant, passing from the left side to the right side of the stable branch and vice versa. The maximal distance from the stable branch is reached when $\sigma = \sigma^*$ ($\dot{\sigma} < 0$ on the left side and $\dot{\sigma} > 0$ on the right side). Therefore, the separatrices denote the maximal libration amplitude.

We now analyze the effects produced by the eccentricity of Jupiter's orbit.

The main effect is that the action N is no longer a constant of motion. N changes on a longer time scale together with the motion of the asteroid's longitude of perihelion and with time (since Jupiter's eccentricity and perihelion change with time). However, the area $-2\pi J$ enclosed by the trajectory during the σ-libration (rigorously defined in Section 2) is an adiabatic invariant. In Figs. 1, 5, 9, and 14, the dashed lines denote some curves J = constant on the (a, e) plane at $\sigma = \sigma^*$. This picture should be interpreted as follows: the dynamics changes slowly, changing the value of N, but in such a way that, any time $\sigma = \sigma^*$, a and e are always on the same dashed line.

The variation of N can have different behaviors (small, large, regular, or chaotic) in the different regions of the phase space. In particular, relevant phenomena can occur near the two secular resonances ν_5 and ν_6. In Figs. 2, 6, 10, and 15 we report the location of these two secular resonances for each mean motion commensurability, the bold solid line denoting the ν_5 and the bold dashed line the ν_6 resonances (in the case of the 4/1 mean motion commensurability only the ν_5 is found). Moreover, the pair of solid lines (for ν_5) and the pair of dashed lines (for ν_6) delimit the amplitudes of the two secular resonances, defined by the location of the corresponding separatrices which are computed by taking only account of one resonance at a time. However, the amplitudes are plotted only when the dynamics associated with the resonance is pendulum-like. This is not always the case, especially concerning the ν_5 resonance in the 4/1 and 7/3 cases. Therefore, Figs. 3, 7, 11, and 16 show the dynamics given by the ν_5 resonance (completely neglecting the ν_6 effect) on different J-level surfaces. These figures can be directly compared with Yoshikawa's (1990, 1991); however, Yoshikawa's figures report $\tilde{\omega} - \tilde{\omega}_J$ on the x axis and the eccentricity on the y axis while ours report $\mathrm{q} = \tilde{\omega} - g_5 t - \sigma^*$ and N. The conversion can be easily made by using the N and J levels plotted in Figs. 1, 5, 9, and 14. The agreement between our results and Yoshikawa's is very good in all cases. At this stage, indeed, our results are equivalent to those provided by the planar elliptic restricted three-body problem.

However, the dynamical effects of the ν_6 resonance and, in particular, the strong interaction between ν_5 and ν_6 cannot be neglected in order to get a realistic picture of the motion. We have therefore dealt with a two-resonance model (see Section 2) that we have integrated numerically. Figures 4, 8, 12, and 17 show several numerical sections of this model. The coordinates reported on the axes are N and $\mathrm{q} = \tilde{\omega} - g_5 t - \sigma^*$, the angle $\mathrm{q} + \sigma^*$ being the critical angle of the ν_5 secular resonance. The section is made on the critical $\mathrm{q}' = \tilde{\omega} - g_6 t - \sigma^* = 0$, the angle $\mathrm{q}' + \sigma^*$ being the critical angle of the ν_6 secular resonance. It is worth noting that, g_5 being the average fre-

quency of Jupiter's longitude of perihelion $\tilde{\omega}_J$ and g_6 the average frequency of Saturn's longitude of perihelion $\tilde{\omega}_S$, the critical angles $q + \sigma^*$ and $q' + \sigma^*$ are usually indicated in the literature as $\tilde{\omega} - \tilde{\omega}_J$ and $\tilde{\omega} - \tilde{\omega}_S$, respectively.

We stress that our surfaces of section are not transversal to the dynamics, namely that they are not Poincaré sections. This is due to the fact that the angle q' may circulate in both directions or librate. However, they are very useful to distinguish chaotic motion from quasi-integrable motion. The lines N = constant and J = constant of Figs. 1, 5, 9, and 14 permit the translation of the results into the original variables a and e.

The numerical sections recall the corresponding Yoshikawa-like figures but, at the stage of the elliptic problem, the secular dynamics turned out to be quasi-integrable. Conversely, taking both secular resonances into account, we can detect the existence of considerable chaos in all the mean motion commensurabilities in study. This strong chaotic behavior is well known from many numerical simulations. In this paper we provide, for the first time, a semianalytical interpretation of this phenomenon. As a matter of fact, few regular regions (of small volume) are still visible in the numerical sections. However, all of them correspond to an eccentricity which is (at least temporarily) sufficient to cross the orbit of Mars. We can imagine that the close encounters with Mars, although not very effective in general (they are effective only on time scales on the order of 10^7 to 10^8 years), can easily kick the asteroids out from these small regular regions and throw them in the surrounding chaotic layer.

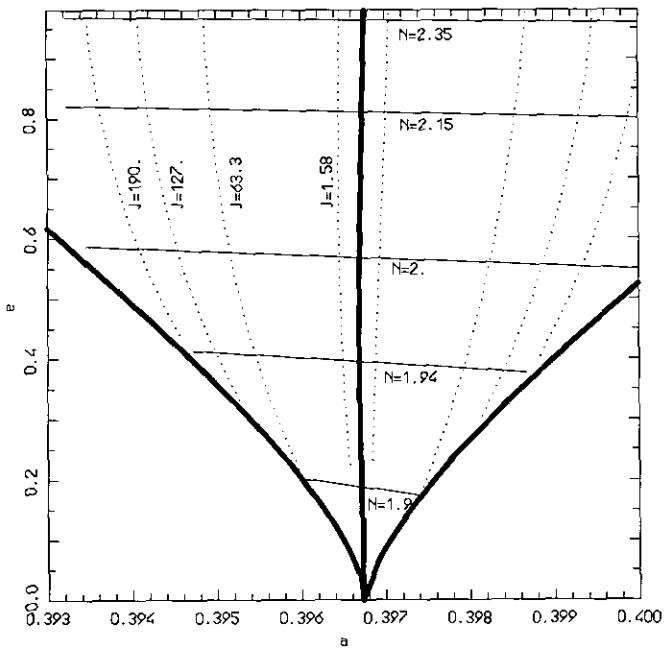

FIG. 1. Dynamics in the 4/1 commensurability: the central thick line is the stable family of periodic orbits of the planar circular restricted problem; the two thick lines on the sides denote the separatrices at $\sigma = 0$; the solid straight lines mark some levels $N = \sqrt{(1-\mu)a}(4 - \sqrt{1-e^2})$ = constant and the dashed lines denote some level J = constant (all J values multiplied by -10^{-5}). The semimajor axis unit is a'.

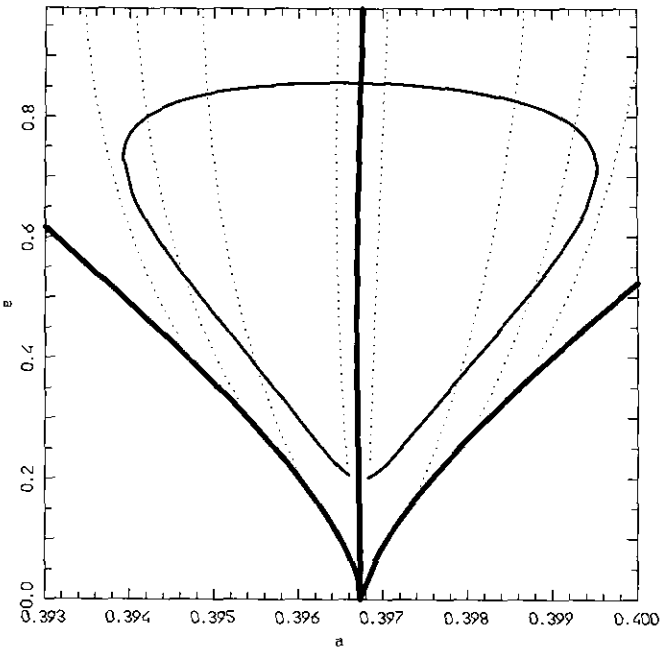

FIG. 2. Secular resonances in the 4/1 commensurability on the plane $i = 0$: the solid bold curve marks the location of the ν_5 resonance; the ν_6 resonance is absent. The dotted lines are the J levels on which the phase space portraits of the ν_5 resonance (Fig. 3) and the numerical integrations of the two-resonance secular model (Fig. 4) are performed.

Since the dynamics turns out to be predominantly chaotic at this stage, which takes into account only the planar motion, we skip the investigation of the dynamics outside the plane. Indeed, the extension of degrees of freedom of the model can only increase the chaoticity of the resulting dynamics, as remarked by Wisdom (1983).

4. THE 4/1 MEAN MOTION COMMENSURABILITY

The 4/1 mean motion commensurability lies at the inner boundary of the main asteroid belt. Assuming the maximum aphelion distance of Mars equal to 1.703 AU and that of Earth equal to 1.058 AU (Quinn *et al.* 1991), the threshold values of the eccentricity to become Mars- and Earth-crossers are respectively 0.175 (N = 1.898) and 0.487 (N = 1.968) (see Fig. 1). As one sees in the Yoshikawa-like pictures of Fig. 3, each orbit is at least forced to reach the value N = 1.94 with the libration/circulation of $\tilde{\omega} - \tilde{\omega}_J$. This mechanism is therefore accepted as the general explanation for the existence of the gap.

As one sees in Fig. 3, the full phase space is dominated by the ν_5 resonance. Each surface J = constant cuts twice the resonance curve (see Fig. 2) and this gives very complicated phase diagrams instead of the typical pendulum-

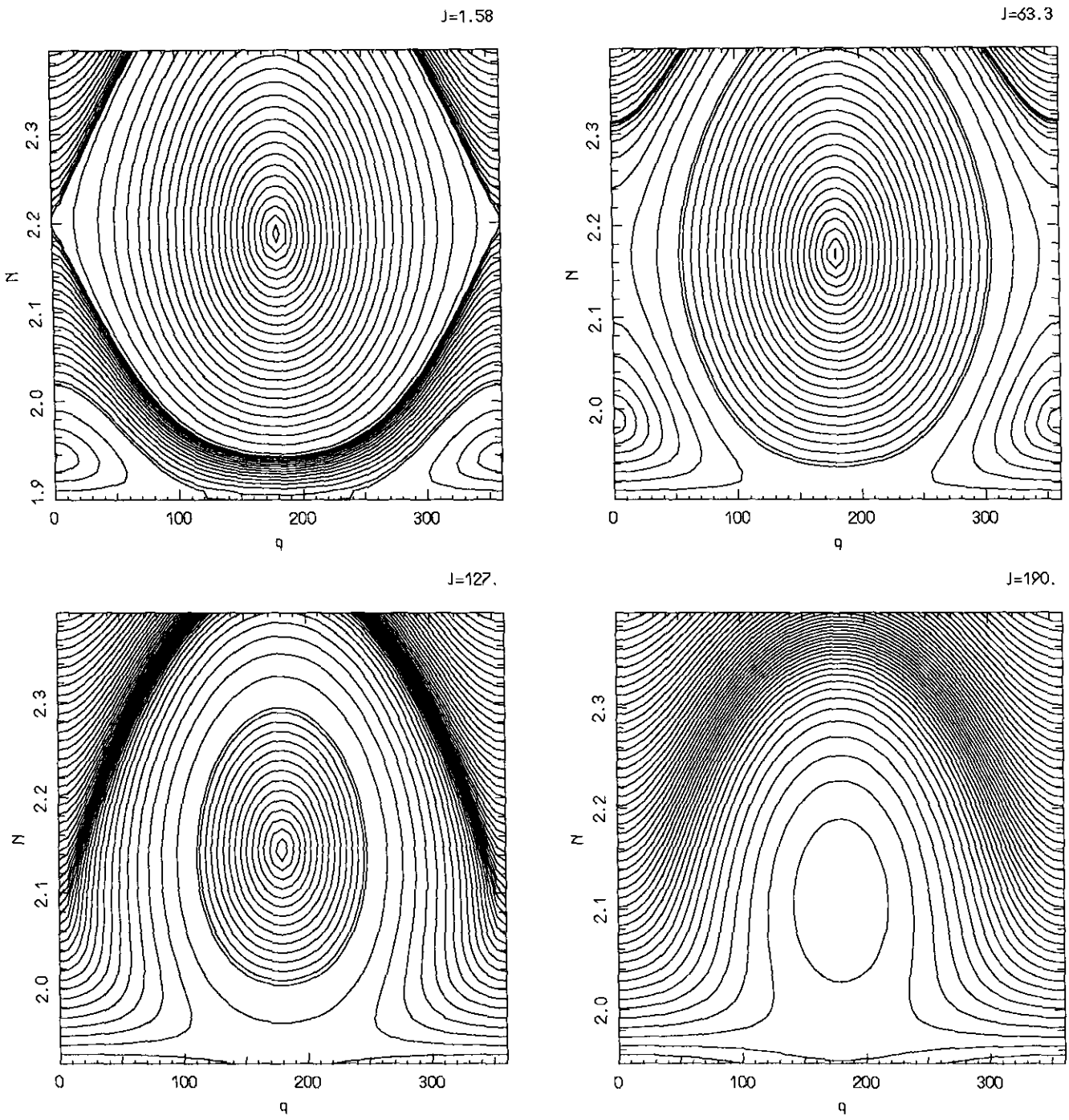

FIG. 3. The phase space diagrams of the ν_5 resonance in the 4/1 commensurability for different values of J (all J values multiplied by -10^{-5}); on the x axis, $q = \bar{\omega} - g_5 t$. These figures are equivalent to those obtained on the basis of the elliptic restricted three-body problem.

like portrait (in the two pictures at the bottom of Fig. 3, for example, the saddle point and the stable equilibrium have the same value of q). Since the ν_5 dynamics is not pendulum-like, in Fig. 2 we have not plotted the location of the separatrices as an indicator of the resonant width since this would not be particularly meaningful.

The 4/1 commensurability is the only one where we cannot find the ν_6 resonance, at least for $0.393 < a < 0.400$ (the unit is $a' = 5.2026$ AU). Therefore this is the mean motion commensurability which has the largest regular regions as shown in Fig. 4 (neglecting, of course, the close encounters with the inner planets). For example, for small amplitude σ-librating orbits (first level $J = -1.58 \times 10^{-5}$) the regular tori fill the phase space up to

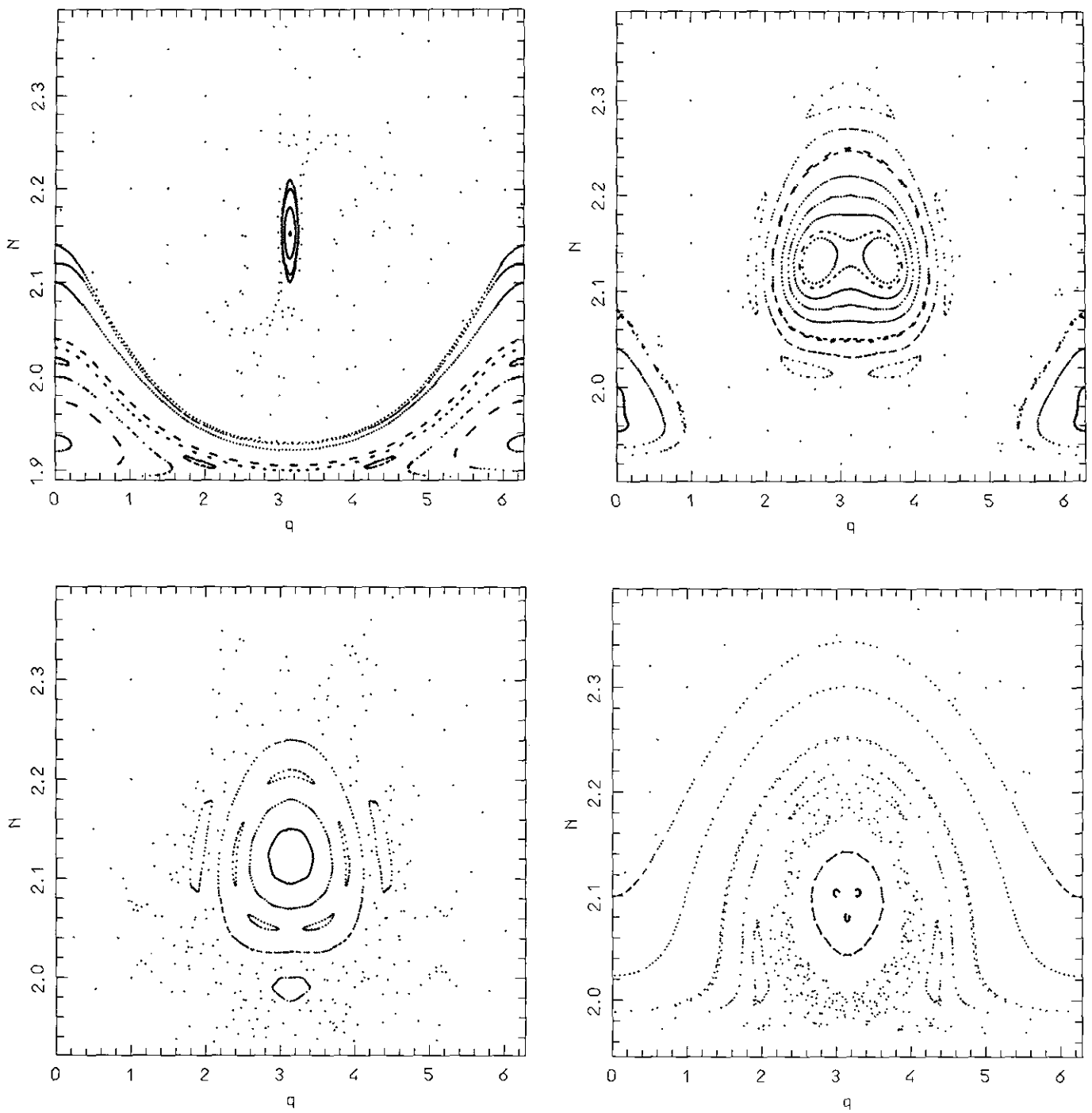

FIG. 4. Surfaces of a section of the numerical integrations of the secular system $\nu_5 + \nu_6$ for the same J levels of Fig. 3. Top left: $J = -1.58 \times 10^{-5}$. Top right: $J = -6.33 \times 10^{-4}$. Bottom left: $J = -1.27 \times 10^{-3}$. Bottom right: $J = -1.90 \times 10^{-3}$.

$N = 1.93$, i.e., $e = 0.36$. However, the existence of the second secular degree of freedom generates a wide chaotic region around the main island where several secondary resonances between the period of libration of $\tilde{\omega} - \tilde{\omega}_J$ and that of circulation of $\tilde{\omega} - \tilde{\omega}_S$ are visible.

5. THE 3/1 MEAN MOTION COMMENSURABILITY

This resonance has been the object of the largest number of studies up to now. Since it is located in the inner part of the asteroid belt, the values of eccentricity which

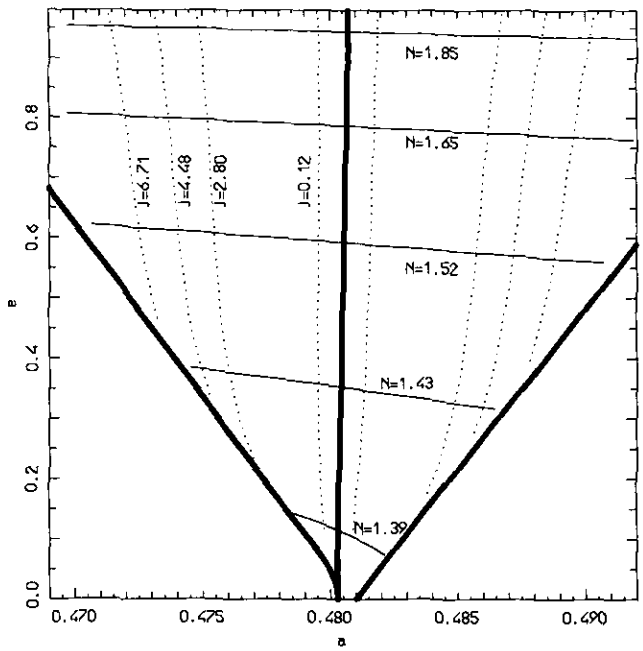

FIG. 5. The same as Fig. 1 for the 3/1 mean motion commensurability; $N = \sqrt{(1-\mu)}a(3 - \sqrt{1-e^2})$ and the separatrices are computed at $\sigma = \pi/2$. The J values are multiplied by -10^{-3}.

are required to cross the orbit of Mars and that of Earth are quite low, i.e., $e = 0.318$ ($N = 1.421$) and $e = 0.577$ ($N = 1.512$) respectively (see Fig. 5).

Since the work of Wisdom (1985) the planar restricted three-body problem has been extensively used in order to explain the existence of the 3/1 Kirkwood gap. Figure 7 summarizes these results. At small $|J|$ (orbits with small amplitude of σ-libration) orbits with starting eccentricity $e = 0.1$ approach the Mars-crossing limit, at least temporarily (bottom of the top left picture of Fig. 7), consistently with the results of Henrard and Caranicolas (1990); the ν_5 resonance is at much larger eccentricity (see also Ferraz-Mello *et al.* 1993). At larger $|J|$ (top right picture of Fig. 7) we can see Wisdom's mechanism in action. A small libration zone appears at moderate eccentricity and q = 0. This libration seems regular in Fig. 7, although one has to recall that the bottom of the picture corresponds to the separatrix of the first degree of freedom (i.e., the σ-resonance of the circular problem); therefore the curves which look tangent to the bottom border are indeed chaotic, and they are the responsible for the famous "Wisdom jumps."

In the 3/1 commensurability, however, the ν_6 resonance is also present and plays a relevant role. As one sees from Fig. 6, the ν_5 and ν_6 resonances largely overlap. Taking both of them together into account in a two-resonance model, we find out that most of the dynamics becomes chaotic (Fig. 8). In particular, the main pendulum-like resonance at large eccentricity is destroyed and only an island of regular motion persists embedded in a large chaotic layer, thus opening the door to large jumps of the eccentricity (up to 0.9). This is typical of what one observes in the pure numerical simulations, rather than the small reversible jumps to $e = 0.3$ first pointed out by Wisdom's mapping.

It is true that, according to Fig. 8, in the region with moderate eccentricity ($N < 1.45$) and small $|J|$, some invariant tori seem to persist. However, along these tori the asteroid has an eccentricity which forces it to cross the orbit of Mars, and we can guess that the encounters with the planet can move it from the invariant torus to the main chaotic region where then the eccentricity goes up to extremely large values; this mechanism could be more efficient than the direct expulsion from the mean motion commensurability due to a close encounter with Mars.

6. THE 5/2 MEAN MOTION COMMENSURABILITY

For this resonance the threshold values of the eccentricity to become Mars- and Earth-crossers are respectively $e = 0.397$ ($N = 1.165$) and $e = 0.625$ ($N = 1.266$) (see Fig. 9). Thus, even in the framework of the restricted three-body problem, and invoking the Mars-crossing depletion mechanism, one can explain the existence of

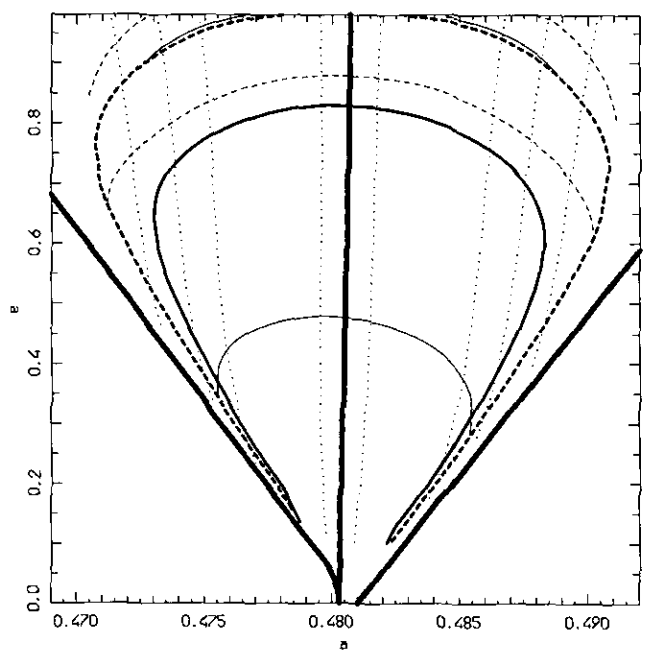

FIG. 6. The same as Fig. 2 for the 3/1 commensurability. In this case also the ν_6 resonance is present (bold dashed curve). The pair of continuous lines and that of dashed lines mark respectively the location of the separatrices of the ν_5 and of the ν_6 resonance.

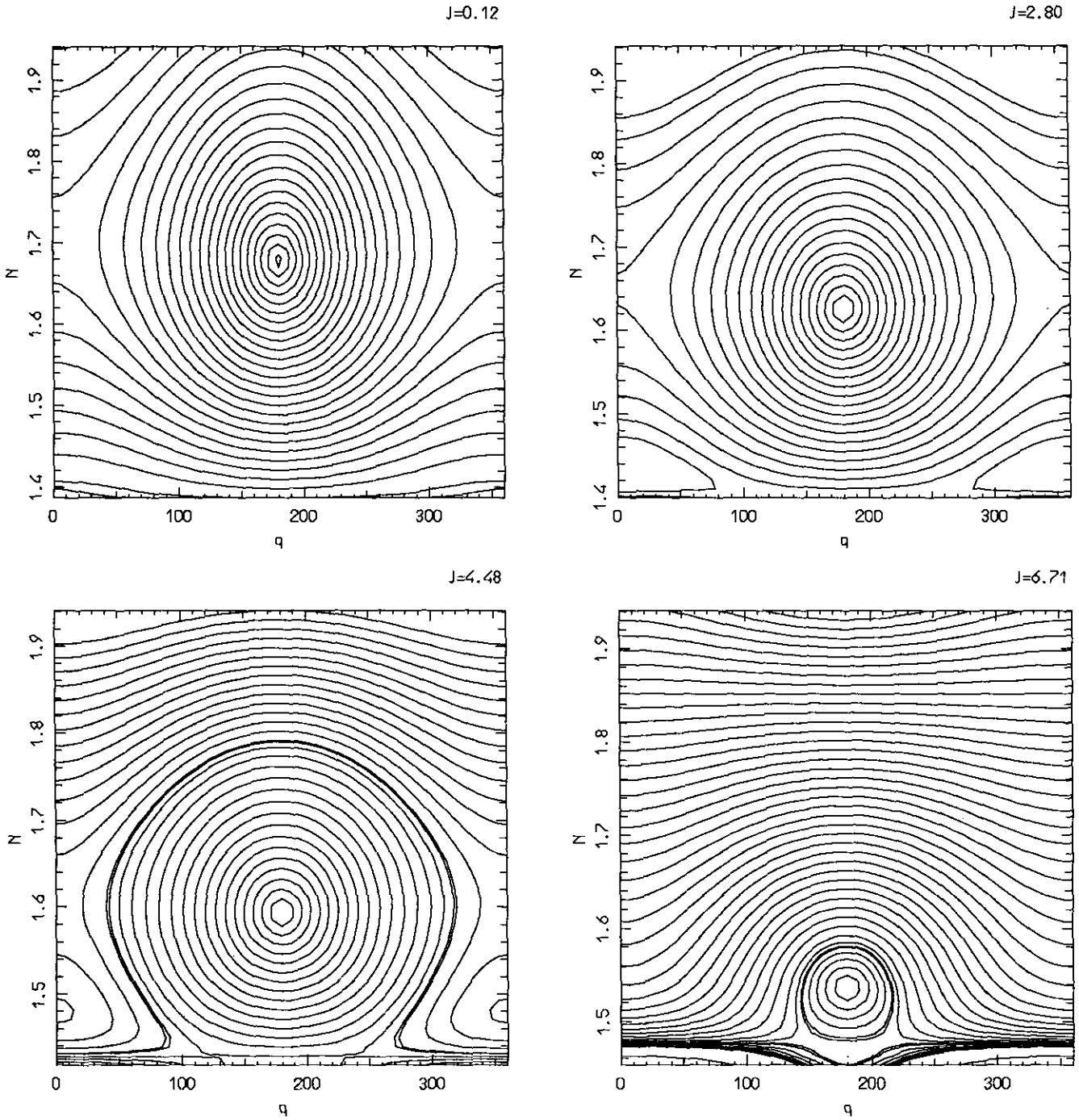

FIG. 7. The phase space diagrams of the ν_5 resonance in the 3/1 commensurability for different values of J (all J values multiplied by -10^{-3}); on the x axis, $\mathrm{q} = \tilde{\omega} - g_5 t - \pi/2$.

this Kirkwood gap, since most orbits come to cross the orbit of Mars. Indeed, looking at Fig. 11 one sees that only asteroids with very small $|J|$ and librating with very small amplitude around the stable equilibrium at $\mathrm{q} = 0$ could escape the Mars encounters.

Taking the full secular problem into account, i.e., including the effects of the ν_6 resonance in our two-resonance model one essentially confirms this scenario. Moreover, we see again (Fig. 12) that large scale chaos is the dominating feature of the dynamics, which is precisely what one typically finds in the pure numerical integrations of fictitious bodies in the 5/2 resonance.

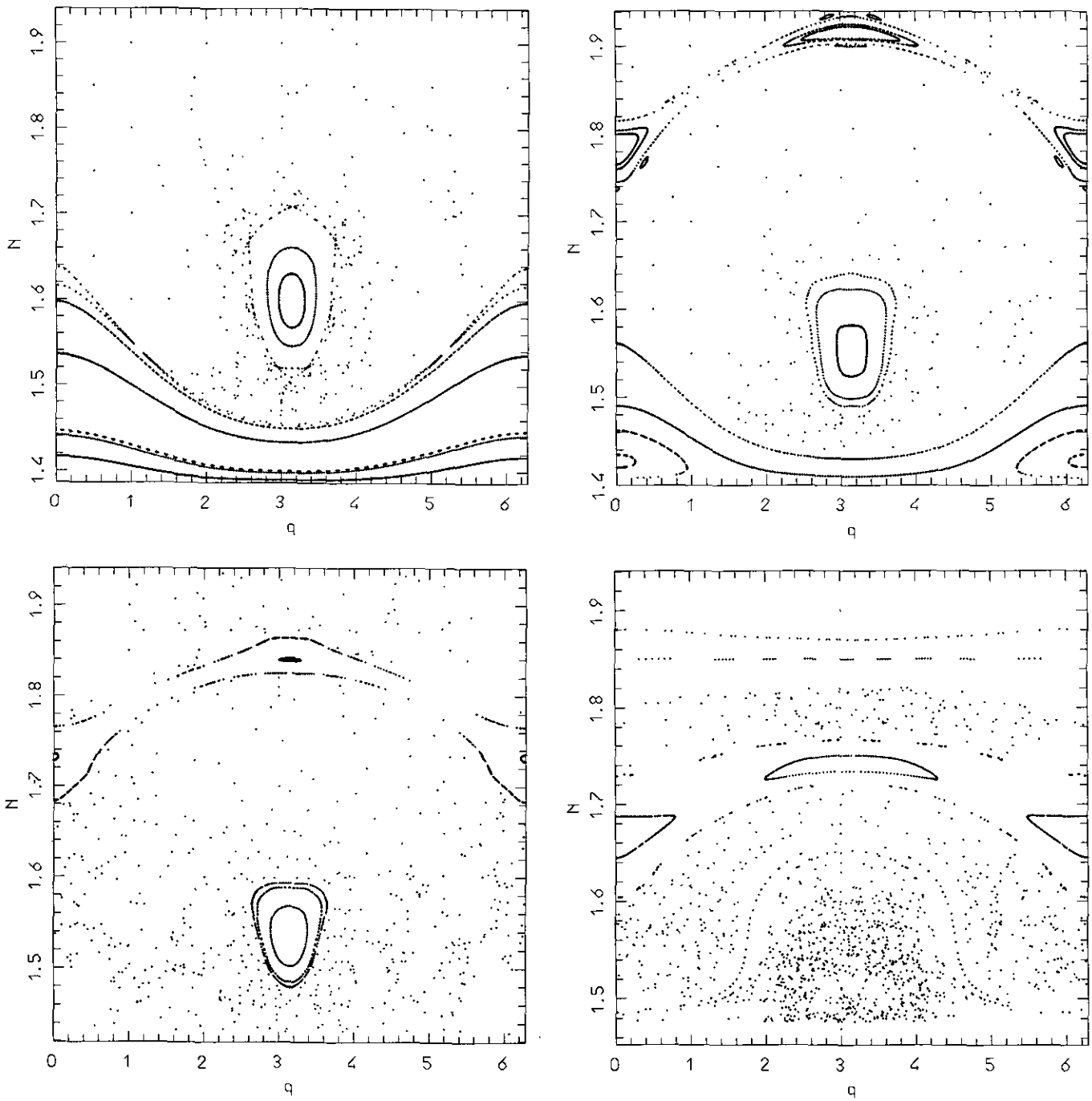

FIG. 8. Surfaces of a section of the numerical integrations of the secular system $\nu_5 + \nu_6$ for the same J levels of Fig. 7. Top left: $J = -0.12 \times 10^{-3}$. Top right: $J = -2.80 \times 10^{-3}$. Bottom left: $J = -4.48 \times 10^{-3}$. Bottom right: $J = -6.71 \times 10^{-3}$.

As a matter of fact, like in the 3/1 case, this large chaotic region does not seem to attain the invariant tori with small N (see bottom of Fig. 12 top left). However, taking into account the encounters with Mars, one can imagine jumps from one torus to the next up to the large chaotic sea. This conjecture is confirmed by the numerical simulation of Fig. 13, which has been kindly provided by R. Gonczi. This shows the evolution of a real object in the 5/2 commensurability, when the full solar system is taken into account. One can observe several regular circulations of the critical angle of the ν_5 resonance $\tilde{\omega} - \tilde{\omega}_J$ associated with oscillations of the eccentricity. The fact that the

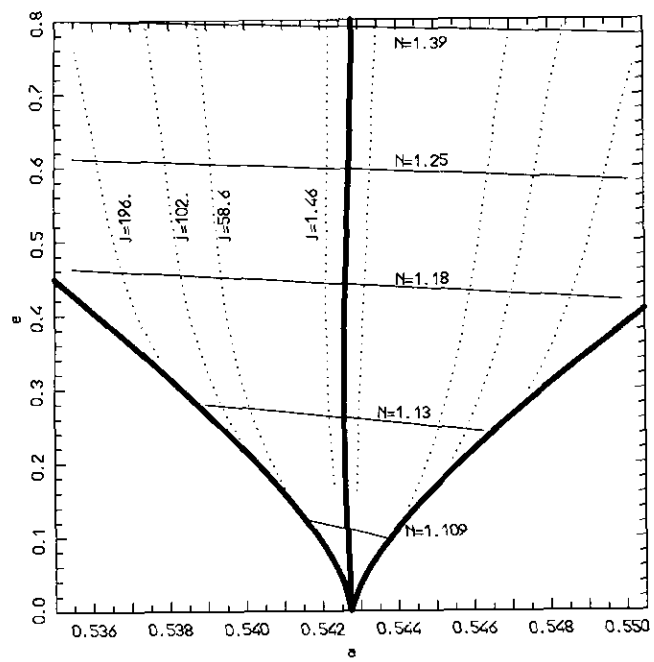

FIG. 9. The same as Fig. 1 for the 5/2 mean motion commensurability; $N = \sqrt{(1-\mu)}a(5/2 - \sqrt{1-e^2})$. The J values are multiplied by -10^{-5}.

amplitude of these oscillations changes proves that the orbit passes from one torus of the secular theory to the other. Finally the orbit is captured in the chaotic region, $\tilde{\omega} - \tilde{\omega}_J$ inverses the direction of motion, and the eccentricity jumps to 1.

7. THE 7/3 MEAN MOTION COMMENSURABILITY

This is the mean motion commensurability with the largest semimajor axis that we analyze here. The threshold values for the eccentricity in order to become Mars- and Earth-crossers are $e = 0.424$ ($N = 1.076$) and $e = 0.642$ ($N = 1.180$) respectively (see Fig. 14). Therefore, in this case the gap cannot simply be explained on the basis of the restricted three-body problem. Indeed, as one sees in Fig. 16, the resonance forces large variations of the eccentricity only on the diagrams corresponding to small $|J|$ (i.e., small amplitude of σ-libration), but, even in these cases, the orbits with $N < 1.02$ (i.e., with $e < 0.15$) are not characterized by large eccentricity changes and therefore never become Mars-crossers.This is indeed the conclusion stated in Yoshikawa's (1991) paper where no definite explanation for the existence of the gap is found.

However, the picture changes completely when the ν_6 resonance is taken into account. In Fig. 17 we report the results of the numerical integration of the two-resonance model. Chaos is the dominating feature up to at least $N = 1.2$, which delimits the region of overlapping between the ν_5 and ν_6 resonances. Only microscopic islands of regular motion persist below this value, which are anyway above the Mars-crossing limit.

As a matter of fact, in some numerical integrations of the Sun–Jupiter–Saturn–asteroid system, Yoshikawa (1989) also found somes cases of large eccentricity variations and chaotic behavior even in the case of wide variation of σ (large $|J|$). We show in this paper that this is not true only for a few trajectories but that large eccentricity variations are a general characteristic of the motion inside of the 7/3 mean motion resonance. We can therefore conclude that the complete secular model makes it possible to explain the origin of this Kirkwood gap.

8. CONCLUSIONS

With this paper we conclude our review on the dynamics in the main mean motion commensurabilities in the asteroid belt. All the commensurabilities analyzed here are associated with evident gaps in the real asteroid distribution. Most of these gaps have been explained in earlier works on the basis of the planar restricted elliptic three-body problem, showing that the eccentricity is pumped

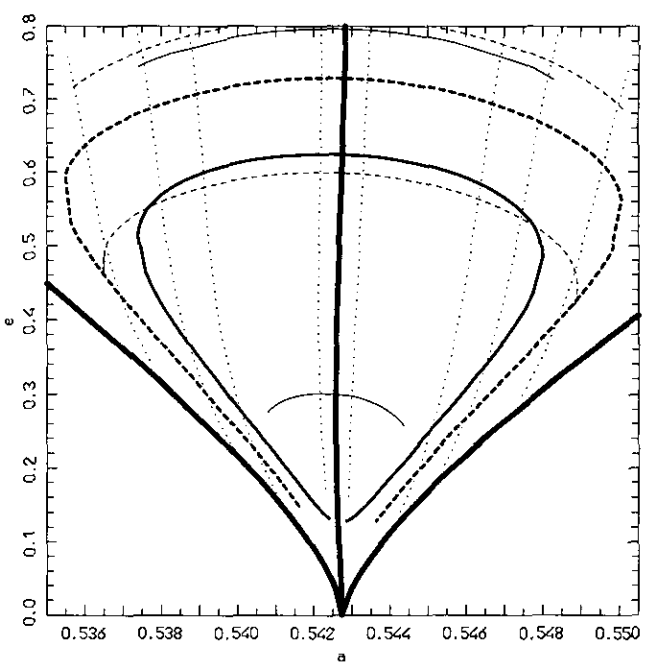

FIG. 10. The same as Fig. 6 for the 5/2 commensurability.

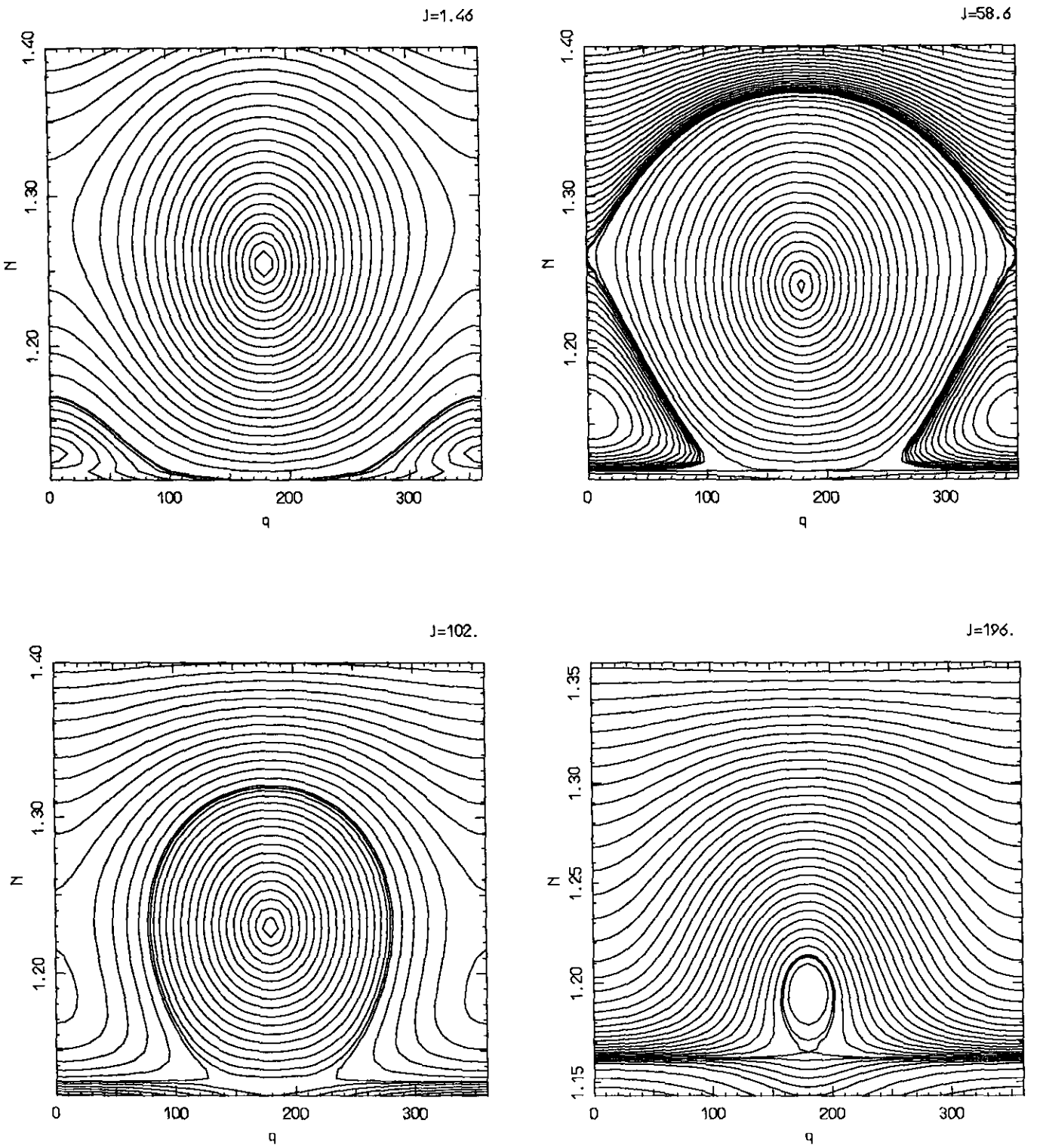

FIG. 11. The phase space diagrams of the ν_5 resonance in the 5/2 commensurability for different values of J (all J values multiplied by -10^{-5}); on the x axis, $q = \bar{\omega} - g_5 t$.

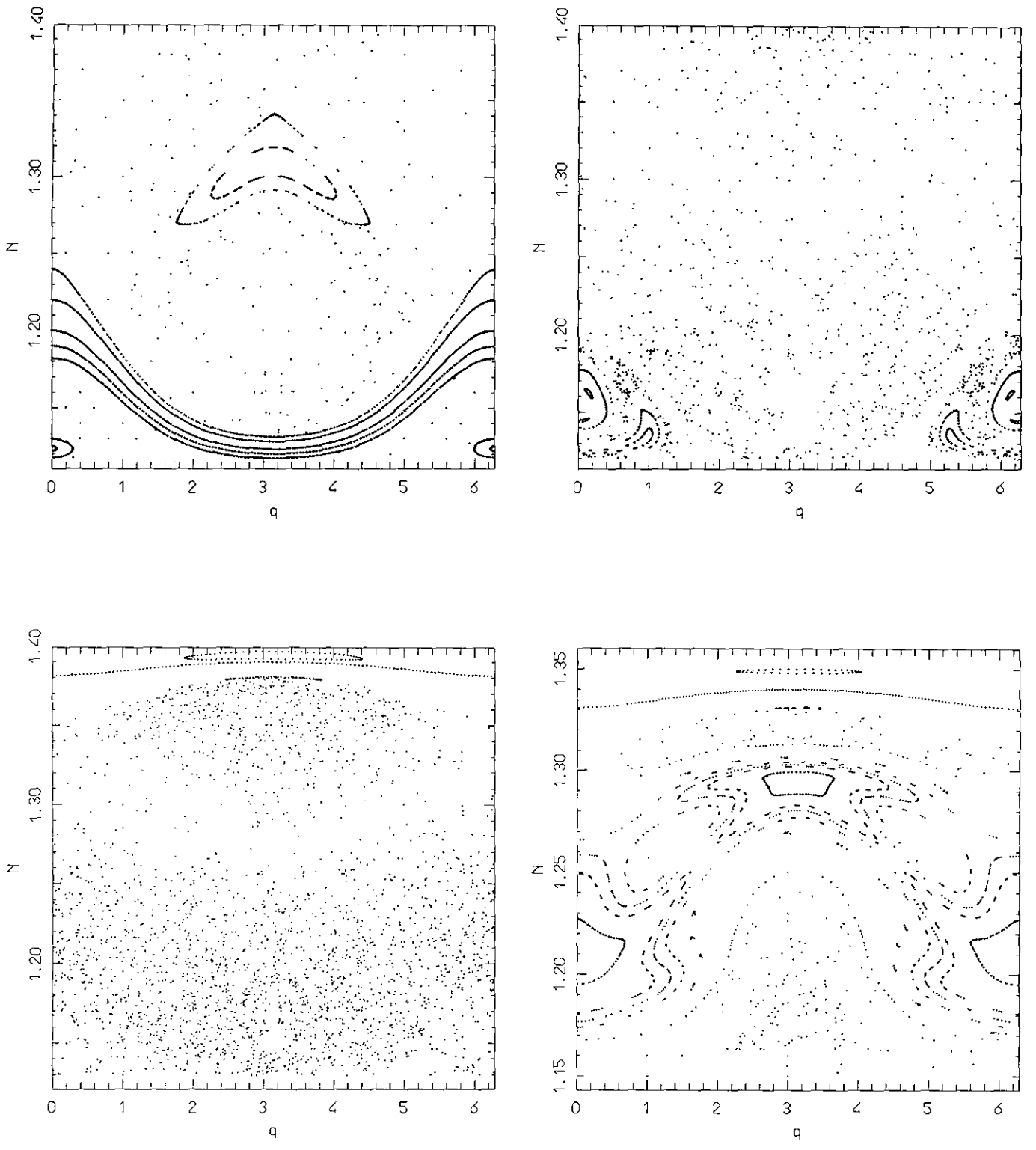

FIG. 12. Surfaces of section of the numerical integrations of the secular system $\nu_5 + \nu_6$ for the same J levels of Fig. 11. Top left: $J = -1.46 \times 10^{-5}$. Top right: $J = -5.86 \times 10^{-4}$. Bottom left: $J = -1.02 \times 10^{-3}$. Bottom right: $J = -1.96 \times 10^{-3}$.

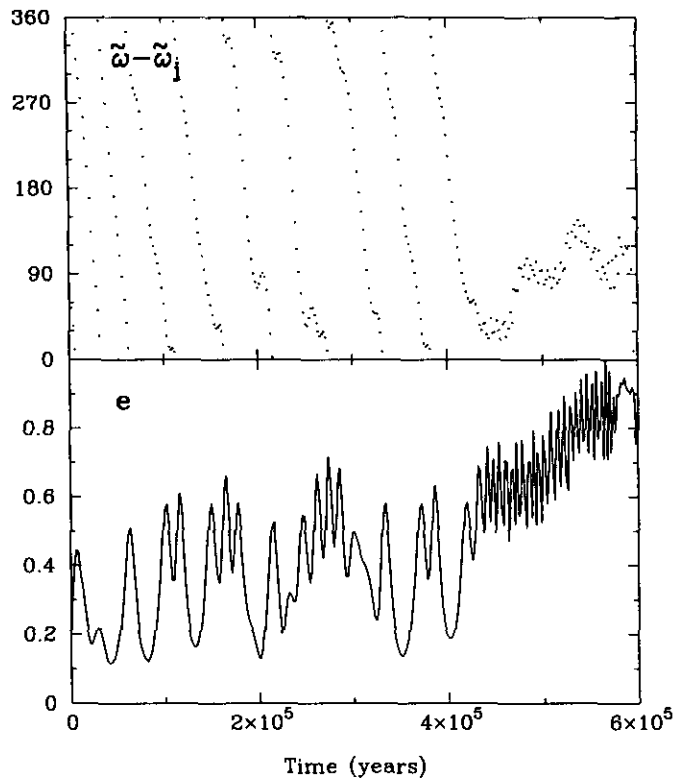

FIG. 13. Results of a numerical integration of asteroid 1991 VP5, taking into account the full Solar System. On the left, the eccentricity as function of time (in years); on the right, the critical argument of the ν_5 secular resonance $\tilde{\omega} - \tilde{\omega}_J$ (in degrees) as function of time (in years). *See text for comments.*

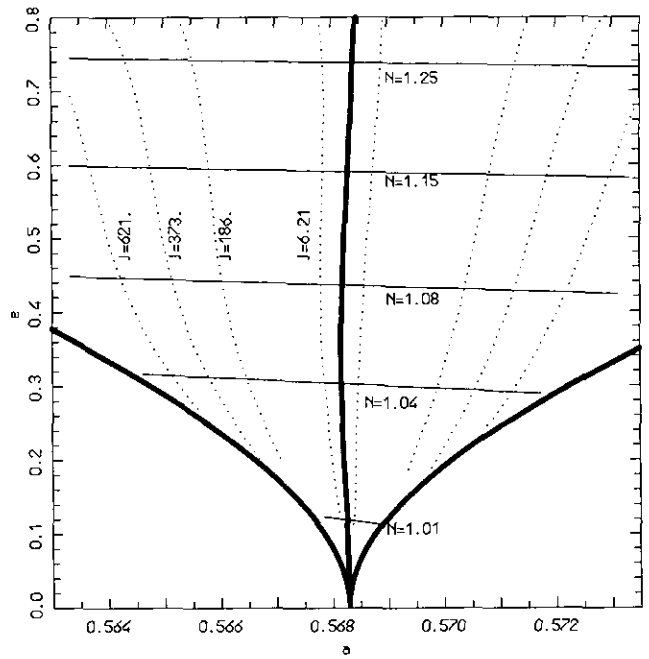

FIG. 14. The same as Fig. 1 for the 7/3 mean motion commensurability; $N = \sqrt{(1-\mu)}a(7/3 - \sqrt{1-e^2})$ and the separatrices are computed at $\sigma = \pi/4$. The J values are multiplied by -10^{-6}.

up to Mars-crossing values, leaving to Mars the job of depleting the commensurability region. However, realistic numerical integrations of fictitious bodies which take into account the perturbations given by the full Solar System show that the orbits in these commensurabilities are wildly chaotic and that the eccentricity wanders up to very large values (~0.8), which leads to encounter not only Mars, but also Earth and, sometimes, Jupiter on a typical time scale of 1 myr. This behavior cannot be explained on the basis of the simple elliptic three-body problem. In this paper we take into account the effects of the secular variations of Jupiter's orbit which are due to the presence of Saturn. We find that the two main secular resonances ν_5 and ν_6 exist inside the mean motion commensurabilities. The interaction and the overlapping between these two resonances generate wide chaotic layers of large scale chaos, which extend up to $e \sim 0.8, 1.0$. In this way we can provide a semianalytic interpretation of the phenomena usually observed and understand the origin of the 7/3 Kirkwood gap.

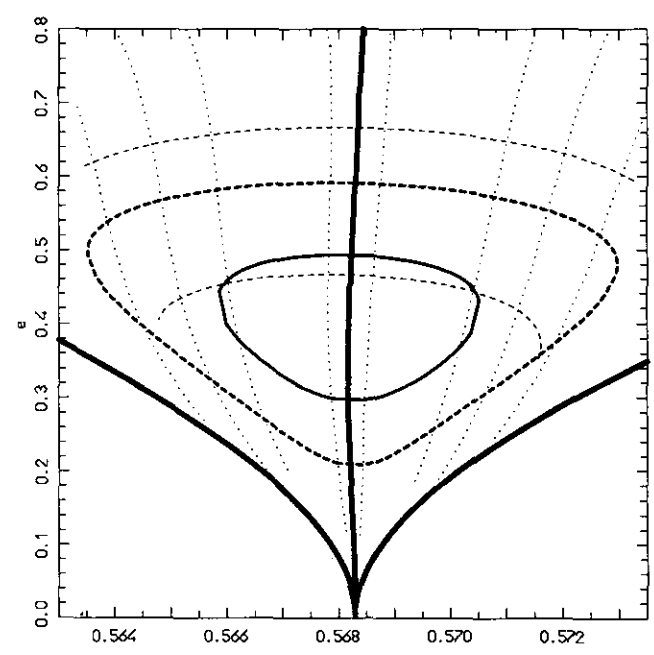

FIG. 15. The same as Fig. 6 for the 7/3 commensurability. The separatrices of the ν_5 resonance are not plotted.

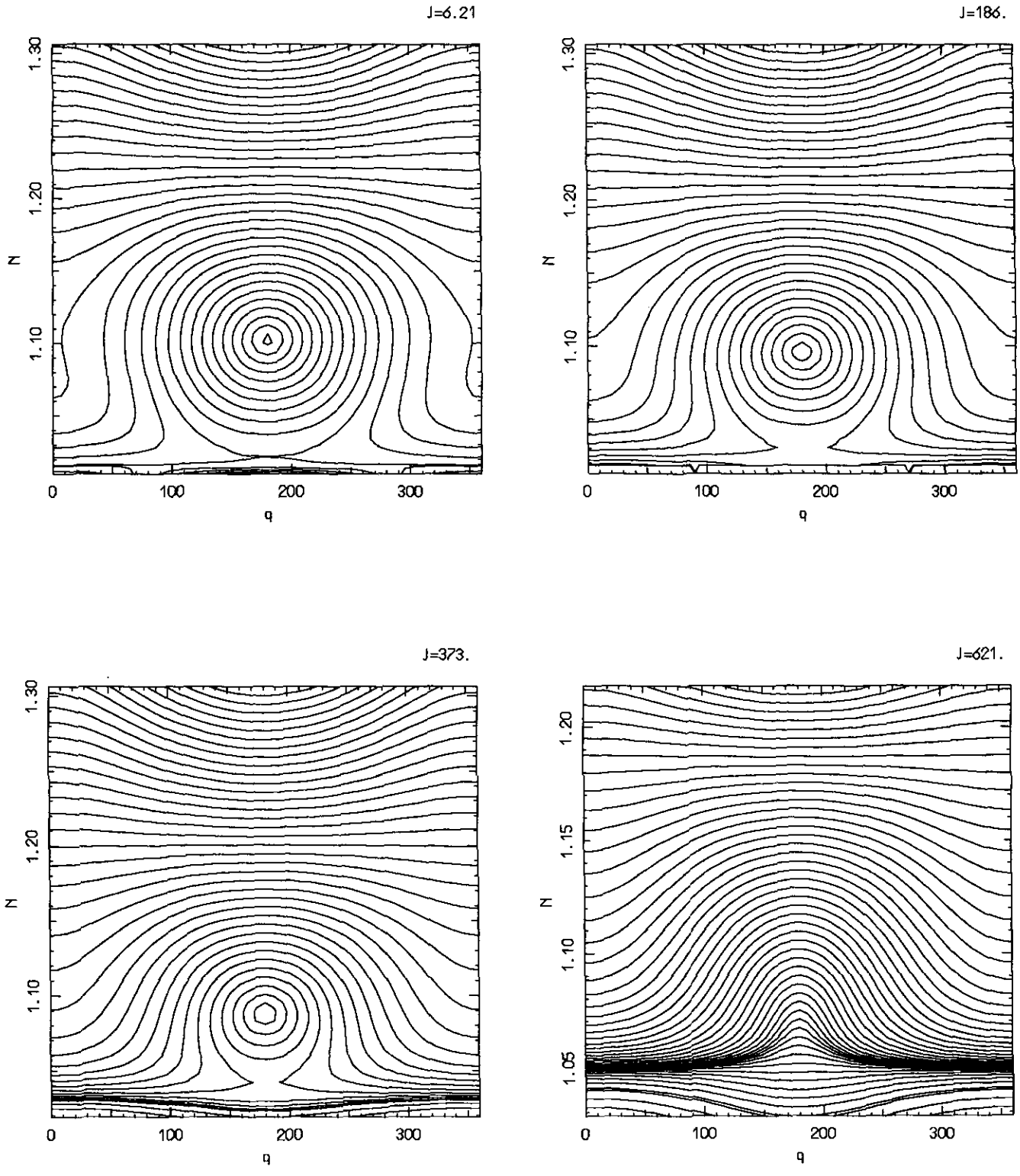

FIG. 16. The phase space diagrams of the ν_5 resonance in the 7/3 commensurability for different values of J (all J values multiplied by -10^{-6}); on the x axis, $\mathrm{q} = \tilde{\omega} - g_5 t - \pi/4$.

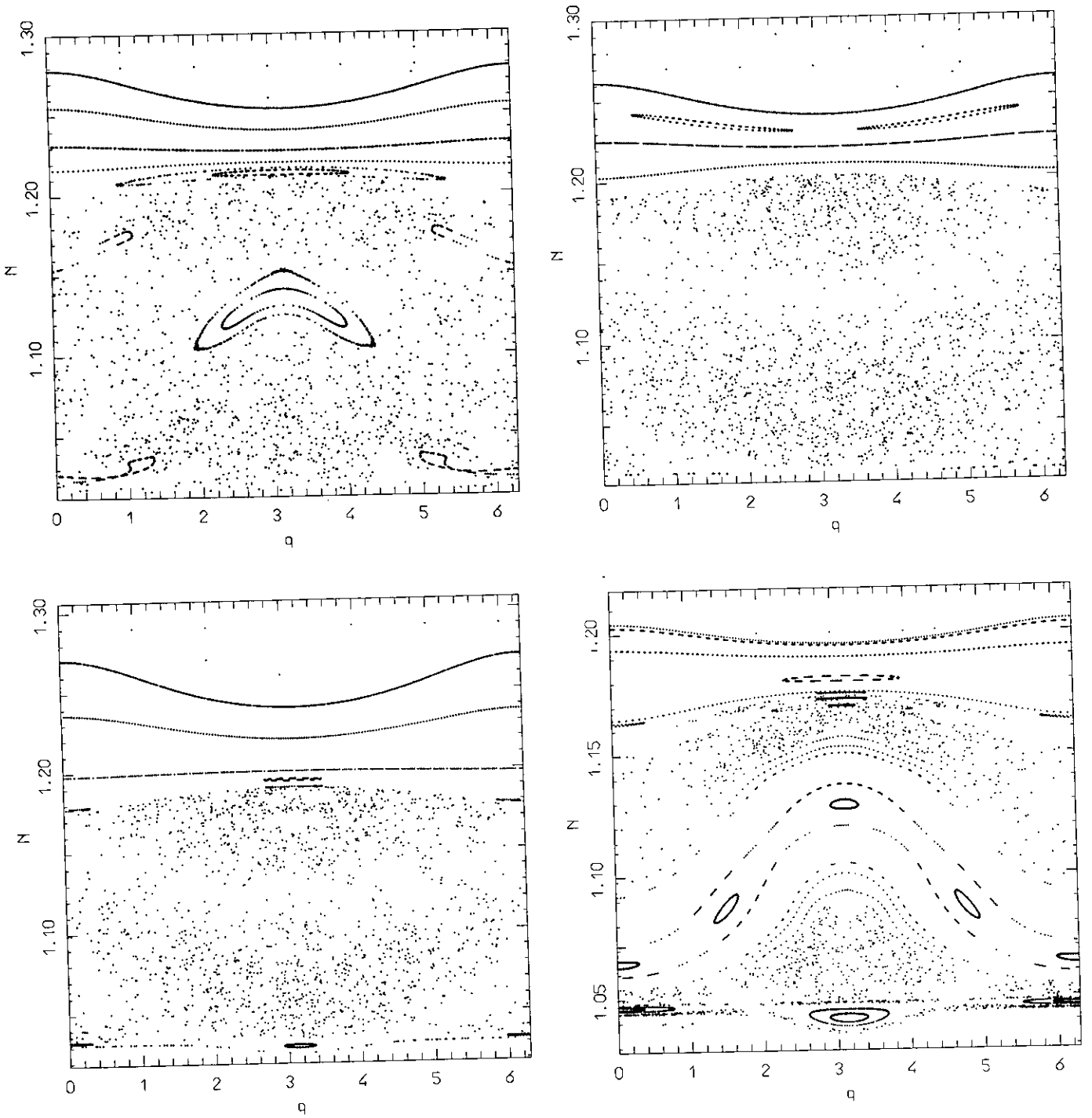

FIG. 17. Surfaces of a section of the numerical integrations of the secular system $\nu_5 + \nu_6$ for the same J levels of Fig. 16. Top left: $J = -6.21 \times 10^{-6}$. Top right: $J = -1.86 \times 10^{-4}$. Bottom left: $J = -3.73 \times 10^{-3}$. Bottom right: $J = -6.21 \times 10^{-3}$.

ACKNOWLEDGMENTS

We are very grateful to J. Henrard, P. Farinella, Ch. Froeschlé, C. Froeschlé, and S. Ferraz-Mello for valuable suggestions. We also thank R. Gonczi for providing us with results of a numerical integration.

REFERENCES

FARINELLA, P., CH. FROESCHLÉ, AND R. GONCZI 1993. Meteorites from the asteroid 6 Hebe. *Celest. Mech.* **56**, 287–305.

FERRAZ-MELLO, S., AND M. SATO 1989. The very-high-eccentricity

asymmetric expansion of the disturbing function near resonances of any order. *Astron. Astrophys.* **225,** 541–547.

FERRAZ-MELLO, S., M. TSUCHIDA, AND J. C. KLAFKE 1993. On symmetrical planetary corotations. *Celest. Mech.* **55,** 25–45.

FROESCHLÉ, C., AND R. GREENBERG 1989. Mean motion resonances. In *Asteroids II* (R. P. Binzel, T. Gehrels, and M. S. Matthews, Eds.) pp. 827–844. Univ. of Arizona Press, Tucson.

FROESCHLÉ, CH., P. FARINELLA, C. FROESCHLÉ, R. GONCZI, G. HAHN, AND A. MORBIDELLI 1995. Secular resonances and dynamics of near Earth asteroids. *Icarus*, submitted.

HENRARD, J. 1990. A semi-numerical perturbation method for separable Hamiltonian systems. *Celest. Mech.* **49,** 43–67.

HENRARD, J., AND N. D. CARANICOLAS 1990. Motion near the 3/1 resonance of the planar elliptic restricted three body problem. *Celest. Mech.* **47,** 99–121.

HENRARD, J., AND A. LEMAITRE 1983. A second fundamental model for resonance. *Celest. Mech.* **30,** 197–218.

LEMAITRE, A. 1984. High order resonances in the restricted three body problem. *Celest. Mech.* **32,** 109–126.

MOONS, M., AND A. MORBIDELLI 1993. The main mean motion commensurabilities in the planar circular and elliptic problem. *Celest. Mech.* **57,** 99–108.

MORBIDELLI, A. 1993. On the successive elimination of perturbation harmonics. *Celest. Mech.* **55,** 101–130.

MORBIDELLI, A., AND M. MOONS 1993. Secular resonances in mean motion commensurabilities: The 2/1 and 3/2 cases. *Icarus* **102,** 316–332.

MORBIDELLI, A., AND M. MOONS 1995. Numerical evidences on the chaotic nature of the 3/1 resonance. *Icarus*, accepted for publication.

NOBILI, A., A. MILANI, AND M. CARPINO 1989. Fundamental frequencies and small divisors in the orbits of the outer planets. *Astron. Astrophys.* **210,** 313–336.

QUINN, T. R., S. TREMAINE, AND M. DUNCAN 1991. A three million year integration of the Earth's orbit. *Astron. J.* **101,** 2287.

SZEBEHELY, V. 1967. *Theory of Orbits.* Academic Press, New York.

WISDOM, J. 1983. Chaotic behavior and the origin of the 3/1 Kirkwood gap. *Icarus* **63,** 272–289.

WISDOM, J. 1985. A perturbative treatment of the motion near the 3/1 commensurability. *Icarus* **63,** 279–282.

YOSHIKAWA, M. 1989. A survey on the motion of asteroids in commensurabilities with Jupiter. *Astron. Astrophys.* **213,** 436–458.

YOSHIKAWA, M. 1990. Motions of asteroids at the Kirkwood gaps. I. On the 3 : 1 resonance with Jupiter. *Icarus* **87,** 78–102.

YOSHIKAWA, M. 1991. Motions of asteroids at the Kirkwood gaps. II. On the 5 : 2, 7 : 3, and 2 : 1 resonances with Jupiter. *Icarus* **92,** 94–117.